Kinematic and Kinetic Gait Features Associated With Mild Cognitive Impairment in Parkinson's Disease

Michela Russo, Marianna Amboni, Antonio Volzone, Sofia Cuoco, Richard Camicioli, Federico Di Filippo, Paolo Barone, Maria Romano, Francesco Amato, and Carlo Ricciardi

***Abstract*— Mild cognitive impairment (MCI) and gait deficits are commonly associated with Parkinson's disease (PD). Early detection of MCI associated with Parkinson's disease (PD-MCI) and its biomarkers is critical to managing disability in PD patients, reducing caregiver burden and healthcare costs. Gait is considered a surrogate marker for cognitive decline in PD. However, gait kinematic and kinetic features in PD-MCI patients remain unknown. This study was designed to explore the difference in gait kinematics and kinetics during single-task and dual-task walking between PD patients with and without MCI. Kinematic and kinetic data of 90 PD patients were collected using 3D motion capture system. Differences in gait kinematic and kinetic gait features between groups were identified by using: first, univariate statistical analysis and then a supervised machine learning analysis. The findings of this study showed that the presence of MCI in PD patients is coupled with kinematic and kinetic deviations of gait cycle which may eventually identify two different phenotypes of the disease. Indeed, as shown by the demographical and clinical comparison between the two groups, PD-MCI patients were older and more impaired. Moreover, PD-MCI kinematic results showed that cognitive dysfunction coexists with more severe axial symptoms and an increase postural flexion. A lack of physiological distal-to-proximal shift in joint kinetics was evidenced in the PD phenotype associated with cognitive impairments.**

***Index Terms*— Gait analysis, kinematics, kinetics, Parkinson's disease, mild cognitive impairments.**

Manuscript received 8 February 2024; revised 18 June 2024; accepted 16 July 2024. Date of publication 19 July 2024; date of current version 29 July 2024. This work was supported in part by the Fondi di Ateneo per la Ricerca di Base (FARB) 2020; and in part by the Rehabilitation Department, University Hospital (A.O.U.) "San Giovanni di Dio e Ruggi d'Aragona," Salerno, Italy, with the Collaboration of M. C. Calabrese, G. Ricciardelli, and M. R. Francese. *(Francesco Amato and Carlo Ricciardi contributed equally to this work.) (Corresponding author: Carlo Ricciardi.)*

This work involved human subjects or animals in its research. Approval of all ethical and experimental procedures and protocols was granted by Campania Sud, the reference ethics committee of the Center for Neurodegenerative Diseases, University of Salerno, and performed in line with the Declaration of Helsinki.

Michela Russo, Maria Romano, Francesco Amato, and Carlo Ricciardi are with the Department of Electrical Engineering and Information Technology, University of Naples Federico II, 80125 Naples, Italy (e-mail: michela.russo2@unina.it; mariarom@unina.it; framato@unina.it; carlo.ricciardi@unina.it).

Marianna Amboni is with the Department of Medicine, Surgery and Dentistry, Scuola Medica Salernitana, University of Salerno, 84081 Baronissi, Italy, and also with IDC Hermitage-Capodimonte, 80145 Naples, Italy (e-mail: mamboni@unisa.it).

Antonio Volzone, Sofia Cuoco, Federico Di Filippo, and Paolo Barone are with the Department of Medicine, Surgery and Dentistry, Scuola Medica Salernitana, University of Salerno, 84081 Baronissi, Italy (e-mail: volzone.antonio95@gmail.com; dott.sofiacuoco@gmail.com; federicodifilippo@hotmail.it; pbarone@unisa.it).

Richard Camicioli is with the Department of Medicine and the Neuroscience and Mental Health Institute, University of Alberta, Edmonton, AB T6G 2R3, Canada.

This article has supplementary downloadable material available at https://doi.org/10.1109/TNSRE.2024.3431234, provided by the authors.

Digital Object Identifier 10.1109/TNSRE.2024.3431234

I. Introduction

PARKINSON'S disease (PD) represents a fast-growing neurodegenerative disease, with a worldwide prevalence of more than 6 million individuals [1]. Neuronal loss in the substantia nigra, leading to a reduction in dopamine production in the striatum, is the neuropathological feature of PD [2]. Moreover, age and gender, genetics and environmental factors may contribute to the pathogenesis of PD [3]. Generally, PD is defined as a motor disease clinically characterised by the presence of bradykinesia in combination with at least one of resting tremor and rigidity. In many cases, PD patients may have other motor deficits, including reduced facial expression, postural instability and gait disturbance, as well as deficits of speech and handwriting [4]. However, a growing body of evidence demonstrated that mental non-motor symptoms are extremely common in PD. These include mood alteration, such as anxiety, depression, lack of motivation and a reduced cognitive capacity, as well as fatigue and sleep disturbance [5], [6].

Cognitive impairment is known to be a common complication, which appears in a large portion of PD patients during the course of the disease. In particular, mild cognitive impairment (MCI) of varying severity is considered an intermediate state between normal cognition and PD dementia (PDD) [7], [8], [9].

Specific neuropsychological tests and cut-off scores are employed to assess the cognitive domains commonly affected in PD, namely executive, attention, memory, language, and visuospatial domains [10]. MCI in PD (PD-MCI) is diagnosed when one or more cognitive domains are affected, without significantly interfering with functional independence [10].

Even though previously MCI was considered a symptom occurring later during the course of PD, several scientific research have shown that PD-MCI can arise in the early stages of the disease [12], [13]. However, PD-MCI prevalence increases while PD advances, thus contributing to reduce the quality of life with the progression of the disease.

Gait analysis, which is used for both clinical purposes and research, provides useful information concerning quantitative gait features which are usually organized in spatiotemporal, kinematic and kinetic parameters [14], [15], [16]. Particularly, kinematic parameters describe angular displacement based on the sagittal, coronal and transverse planes for various joints such as the ankle, knee, hip and pelvis area, while kinetic parameters give details on the forces and their effect on motion [17]. A few studies have also evaluated whole body kinematics in healthy and pathological populations, using new marker set protocols involving head, upper limb and spinal curves in orthostatic posture [18] and during walking [19], [20]. Indeed, there has been a significant progress in the use of gait analysis both to quantitatively evaluate the relationship between executive functions and walking in healthy population [21], [22].

Recent findings reveal that gait analysis can be considered as an effective strategy for monitoring and assessing the nature and the severity of the disease, by distinguishing different PD phenotypes as well as different types of parkinsonism [23], [24], [25], [26]. Furthermore, gait is no longer considered an automated motor task but an activity where executive function, attention and visuospatial abilities play an important role [27]. Alterations in one or more of these cognitive domains may contribute to gait disturbances. Therefore, the interplay between cognitive impairment and gait abnormalities has received increasing attention in the last few decades. Indeed, there has been a significant progress in the use of gait analysis for identifying gait parameters which are strongly correlated with PD-MCI [28], [29], [30], [31].

In previous studies, spatiotemporal parameters of PD patients with and without MCI (PD-MCI and PD-noMCI, respectively) have been widely investigated. The findings have supported the notion that PD-MCI patients show higher postural instability and gait disorders than PD-noMCI, especially during a dual-task [29], [32].

A growing number of studies have investigated changes in gait kinematic and kinetic parameters of PD patients during different gait conditions [33]. Most of them describe the kinematic and kinetic patterns of PD patients, with particular attention on the ankle joint. Morris et al. assessed the gait parameters of a PD patient during various conditions. The patient was able to improve the kinematic parameters with the aid of an external visual cue, but he continued to show abnormality in the kinetics, such as a reduced ankle power generation at push-off [34]. Lewis et al. observed a reduced ankle plantarflexion at toe-off and reduced ankle power generation at baseline when comparing PD patients with age-matched healthy subjects [35].

The use of machine learning (ML) approaches for the automated recognition of gait-pattern has been growing exponentially [36], [37], [38]. An increasing number of studies is employing ML models on spatiotemporal gait parameters for the recognition of PD, the classification of different PD stages and the identification of a subset of spatiotemporal variables that could reliably describe the relationship between cognitive domains and gait [39], [40], [41], [42].

However, the automated classification on gait kinematic and kinetic parameters in PD has been poorly discussed in the previous literature. Martinez et al. used pressure insoles to quantify force characteristics of mild PD patients during the *On clinical* status and reached a classification accuracy of 64.1% using discriminant analysis [43]. Tahir et al. classified PD gait and normal subjects using kinematic and kinetic parameters as input of an artificial neural network. An accuracy of 68.8% was reached for the kinematic parameters and 71.9% for both the kinetic parameters and the fusion of the two [44].

In the present study, the gait analysis of a large cohort of PD patients was assessed using a 3D optoelectronic system. An ad hoc software was implemented to extract specific kinematic and kinetic parameters of walking (including angular joint motions, pelvis and trunk movements, ground reaction forces (GRF), joint moment and power) during three different gait conditions: single-task (i.e., free walking only), motor dual-task and cognitive dual-task.

The aim of this scientific study was two-fold:

1. The assessment of the interactions between gait kinematic and kinetic parameters in single and dual-task of PD-MCI and PD-noMCI patients in order to confirm the hypotheses that PD-MCI and PD-noMCI have different gait-patterns not only in terms of spatiotemporal parameters, as widely investigated [24], [25], [28], [35], [36], [40], but also in terms of kinematic and kinetic parameters. The analysis was performed on both the complete dataset including 90 patients and a reduced age-matched dataset including 47 patients in order to further demonstrate the independence of our findings from age.

2. The use of date-driven ML-based approaches to test the hypothesis that gait kinematic and kinetic parameters can be useful to discriminate PD-MCI from PD-noMCI.

II. Methods

A. Study Population

The overall study population was composed by 90 PD patients consecutively enrolled at the Center for Neurodegenerative Diseases of the University of Salerno, Italy, based on inclusion and exclusion criteria published elsewhere [41]. The diagnosis of PD was confirmed by a movement disorder specialist according to the MDS clinical diagnostic criteria for PD [45]. The severity of motor and non-motor symptoms of PD patients was evaluated using the four parts of the Movement Disorder Society Unified Parkinson's Disease Rating Scale (MDS-UPDRS) [45]. Disease staging was assessed with Hoehn & Yahr (H&Y) scale [46]. According to the MDS diagnostic criteria for MCI in PD, among enrolled patients, 40 of the enrolled patients were PD-MCI and the rest were PD-noMCI [11]. For each PD patient, the main clinical and demographic characteristics were recorded to evaluate patients' clinical conditions: age, body mass index (BMI),

disease duration, levodopa-equivalent daily dose (LEDD), H&Y score and MDS-UPDRS (for each subscore and total score).

B. System Description

Gait kinematic and kinetic variables were assessed while patients were during the *On* state. Kinematic data were recorded using an optoelectronic system (SMART-DX 400, BTS-Bioengineering, Italy), consisting of six video cameras working at a sampling rate of 100 Hz and located around a calibrated volume of 8 m x 5 m x 3 m. Anthropometric measurements were taken for each subject and then 22 passive retro-reflective markerswith a diameter of 14 mm were attached bilaterally to the following bony landmarks, according to Davis protocol [47]: the acromion, anterior superior iliac spine, great trochanter, lateral femoral condyle, fibula head, lateral malleoli, metatarsal head, and heel. Individual markers were attached between the 2nd and 3rd sacral vertebras, and on the 7th cervical vertebra. Moreover, sticks markers were placed at 1/3 of the length of femur and leg segments. These measurements were used for the estimation of internal joint centers and allowed to calculate the kinematics of the trunk and lower limb.

Kinetic data were measured by means of two platforms (60 cm x 40 cm) embedded in the middle of a 3m walkway. Both platforms were positioned one by one, and the participants positioned one foot per force plats.

C. Experimental Procedure

The gait tests were performed during the *On* state of the medication cycle (1-2h after taking the morning dose), with a double aim: 1. To reduce the confounding role of different motor states; 2. To capture dopamine-resistant gait dysfunctions, being these ones more strictly associated with cognitive decline in PD [29], [32], [48]. Subjects were instructed to walk at their usual self-selected speed and performed three experimental gait tasks: a single task (normal walking (GAIT)) and two commonly employed dual-task procedures (motor and cognitive dual-task) [49], [50]. In the motor dual-task (MOT), subjects walked at their self-selected speed while carrying a tray with 2 glasses filled with water. In the cognitive dual-task (COG), subjects walked at their self-selected speed while serially subtracting the number 7 starting from 100. All patients completed four walking trials for each task from which spatiotemporal, kinematic, and kinetic data were computed. For each subject, the mean of the four trials was calculated to improve the reliability of the data.

D. Data Elaboration

Dedicated software (Smart Clinic, BTS Bioengineering, Milan, Italy) was used to define gait cycle events and to process raw data. The kinematic movements of joints based on sagittal, coronal and transverse planes were computed. Particularly, trunk and pelvic tilt, hip and knee flexion-extension and ankle dorsi-plantarflexion were extracted on the sagittal plane. Trunk and pelvic obliquity and hip adduction-abduction were computed on coronal plane. Finally, trunk and pelvic area, and hip and knee rotation were computed on transversal plane. GRF were recorded, by walking on the force plates.

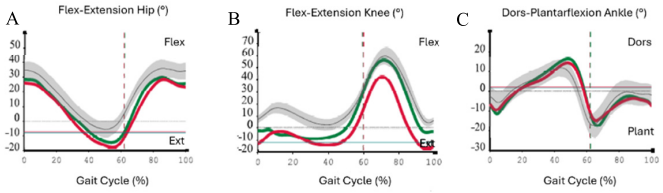

Fig. 1. Kinematic data at (A)hip, (B) knee and (C) ankle across the gait cycle. Positive angles point out joint flexion and dorsiflexion, while negative angles indicate extension and plantarflexion. The red line represents the left signal; the green line represents the right signal, and the grey area represents control range. The vertical line shows the transition from the stance to the swing phase.

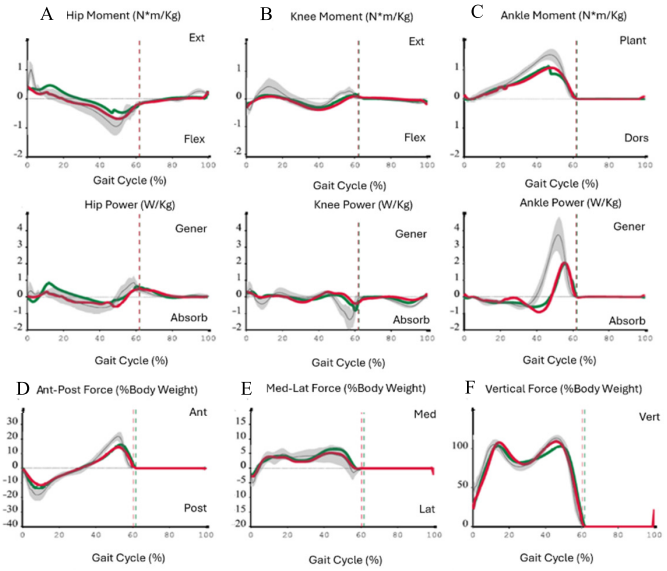

Fig. 2. Kinetic data at (A) hip, (B) knee and (C) ankle across the gait cycle. Positive angles point out joint extension and plantarflexion, while negative angles indicate flexion and dorsiflexion. The red line represents the left signal; the green line represents the right signal, and the grey area represents control range. Ground reaction force at (D) antero-posterior, (E) medio-lateral and (F) vertical. The vertical line shows the transition from the stance to the swing phase.

In addition, joint internal moments (M) and powers (P) were computed by combining kinematic and kinetic parameters. These data were normalized with respect to the subject's body mass (in kilograms):

$$\text{Normalized M} = \frac{Moment(N*m)}{Body\ weight\ (Kg)} \quad (1)$$

$$\text{Normalized P} = \frac{Power(W)}{Body\ weight(Kg)} \quad (2)$$

For each of the joint movements, Smart Clinic software extracted the right and left gait signals, as shown in Fig 1 and Fig 2.

The right and left signals of the joint movements were given in input to an ad hoc algorithm implemented in MATLAB (v.R2023a) for the computation of the quantitative kinematic

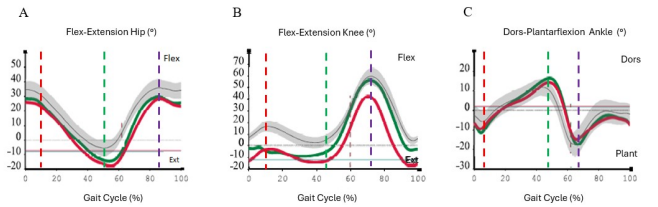

Fig. 3. Graphical representation of gait cycle phases for A) Hip, B) Knee and C) Ankle joints. The vertical red line represents initial contact phase, the vertical green line represents mid-stance phase, and the vertical blue line represents mid-swing phase.

and kinetic parameters of each task (GAIT, MOT & COG) during specific gait cycle phases (Fig 3). The algorithm consisted of the following steps:

1. The right and left gait signals (Fig 1 and Fig 2) of each joint movement were averaged and a MEANSignal was obtained.
2. Specific gait cycle phases were individuated in MEANSignal (Fig 3):
   - Initial contact was defined as the frame in which the subjects' heel first came in contact with the floor. Generally, it is in the first 10% of gait cycle.
   - Stance phase was defined as the frame in which the subjects' foot is in contact with the floor. Generally, it is between 20% and 60% of gait cycle.
   - Swing phase was defined as the entire frame in which subjects' foot is in the air. Generally, it is between 60% and 80% of gait cycle.
3. The maximum and minimum of each MEANSignal were computed in the above-mentioned gait cycle phases (Fig 3).
4. Range of Motion (ROM) was obtained as the difference between the maximum and minimum angle of movement that a joint can make during the gait cycle.

Regarding the kinematic variables, the following were computed: maximum and minimum of the pelvic tilt (anteversum/retroversum, respectively), rotation (internal/external, respectively) and obliquity (high and low, respectively); the maximum (at initial contact and in swing phase) and minimum (in stance phase) of the hip flexion-extension, adduction-abduction and internal/external rotation; maximum (at initial contact and in swing phase) and minimum (at stance phase) of the knee flexion-extension and internal/external rotation, and maximum (at stance phase) and minimum (at initial contact and swing phase) of the ankle dorsi-plantarflexion (Fig 3). Additionally, ROM was estimated for hip and knee flexion-extension and ankle dorsi-plantarflexion.

Regarding the kinetic variables, the following were computed: moment in flexion-extension (at stance phase) for hip and knee joint, moment in flexion-extension (at loading response and at stance phase) for ankle joint; power generated and absorbed in stance phase for each joint and the medio-lateral (M-L), antero-posterior (A-P) and vertical (V) GRF.

Finally, an entire dataset with 45 quantitative kinematic parameters and 15 quantitative kinetic parameters was obtained for each task (GAIT, MOT & COG). Fig 4 shows the 3D reconstruction of the patient in a calibrated volume in the sagittal and frontal plane.

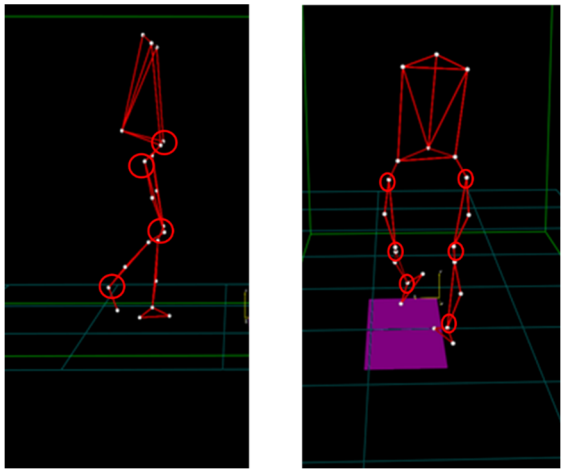

Fig. 4. Patient 3D reconstruction in a calibrated volume in the sagittal and frontal plane. Red circles show the angular joint movements for hip, knee and ankle.

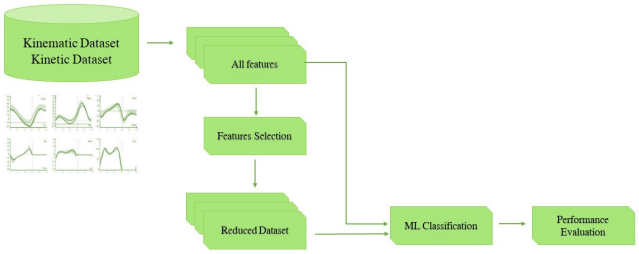

Fig. 5. Workflow of the ML analysis.

E. Statistical Analysis

A univariate statistical analysis was conducted by using SPSS. The Kolmogorov-Smirnov test and the Levene's test were used to evaluate the normality distribution of the data and the homoscedasticity of variances between groups for normally distributed data, respectively. The normally distributed data underwent a t-test for independent samples; otherwise, a Mann-Whitney test was employed [51]. An $\alpha = 0{,}05$ significance level was used on clinical and demographical variables and on kinematic and kinetic parameters in order to find differences between PD-MCI and PD-noMCI patients.

F. Classification and Features Selection

Statistical analysis was followed by a supervised ML approach which was implemented with MATLAB (v. R2023a). Fig 5 shows the ML workflow.

At the beginning, a classification analysis was conducted separately on kinematic and kinetic parameters for each single task (GAIT, MOT & COG). Based on literature [41], [52], [53], [54], different ML algorithms widely reported in the classification of PD gait analysis were employed. In the current study, seven classifiers based on various mathematical principles were used in order to determine which one performed the best results on gait data. Algorithms used gait kinematic and kinetic parameters as predictor variables and disease cognitive status (PD-MCI or PD-noMCI) as responsible variable. Leave-one-out cross validation (LOO-CV) was performed to validate the predictive algorithms.

LOO-CV is a special case of k-fold cross validation, where the number of folds is equal to the number of instances in the dataset [55]. This effectively resulted in 'k=90' folds, where 'k' represents the total number of data points. Thus, ML algorithm is applied for each instance belonging to the dataset, which is used as a test-set while all other instances are used as a training set [56].

The ML algorithms are briefly reviewed as follow:

- Decision Tree (DT) is the easiest non-parametric algorithm know in literature due to its simplicity, interpretability and effectiveness. Indeed, DT does not require much effort for data preparation and the normalization of data is not always required. Input data are recursively split into roots while leaves represent class labels [57], [58].
- Random Forest (RF) is the most popular ML algorithms that belongs to the family of ensemble methods. RF is a combination of DT classifiers where the random vectors generated for each tree are identically distributed and each tree has a response variable for each input. Once the trees are grown, the most recurrent response variable is applied to the outputs (i.e., class labels) [57], [59].
- Gradient boosted tree (GBT) is a tree-based algorithm that belongs to ensemble ML classifiers. The principle of this algorithm is to turn weak learners (weak decision trees) into strong learners that predict with greater accuracy. Each single tree is added to the model and each one is built considering the errors of previous trees [57].
- Support Vector Machine (SVM) is a ML algorithm widely used because of its high performance. The underlying idea of SVM classifiers is to find the best hyperplane that separates two classes of the data. The best hyperplane refers to the one with the largest distance between the two classes [57], [60].
- K-nearest neighbours (KNN) is another non-parametric algorithm for the classification. The principle of KNN is that each instance is classified based on the closest training samples present in the space. To determine the nearest points or the closest groups can be used a distance metric, such as the Euclidean distance or Manhattan distance [57].
- Linear Discriminant Analysis (LDA), in a binary analysis, is a ML algorithm used to find a linear combination of features that characterizes or separates two classes of samples. LDA works by modelling the distribution of each class using Gaussian distribution. LDA is computationally efficient with high-dimensional data using a small number of training samples [57].
- Naïve-Bayes (NB) is one of the ML algorithms belonging to the family of "probabilistic classifiers" based on applying Bayes theorem. This algorithm works by computing the probability of each class, and then selecting the class with the highest probability as the predicted class [57], [61].

The very large number of kinematic (N=45) and kinetic parameters (N=15) may lead to overfitting due to the dataset dimensionality. Therefore, feature selection methods offer an advanced approach to select information-full feature subset [62].

In this study, a subsequent investigation by employing features selection method was used on the entire dataset to reduce the dimensionality of the data and find the best subset of kinematic and kinetic features among the three gait tasks [62], [63]. For this second analysis, as a preliminary step, a hold-out cross validation was used to split the dataset into training (80%) and testing (20%), and then the wrapper feature selection method was employed. Wrapper method starts training by using a subset of features and then adds or removes a feature to select the best subset of features to the optimal results [62].

Finally, the performance of the proposed algorithms was evaluated through several metrics [64]:

- *Specificity (Sp)*: capacity to correctly detect subjects not belonging to the group under examination:

$$Sp = \frac{TN}{TN + FP}\,(\%) \tag{3}$$

- *Sensitivity (Se)*: capacity to detect correctly subjects belonging to the group under examination:

$$Se = \frac{TP}{TP + FN}\,(\%) \tag{4}$$

- *Precision (Pr)*: a measure of the positive patterns correctly predicted from the total predicted patterns in a positive class:

$$Pr = \frac{TP}{TP + FP}\,(\%) \tag{5}$$

- *Accuracy (Ac)*: the ratio of correct predictions over the total number of records:

$$Ac = \frac{TP + TN}{TN + FP + FN + TP}\,(\%) \tag{6}$$

where TP, TN, FN, and FP denote true positives, true negatives, false positives, and false negatives, respectively.

In addition, we used a further metric, namely the Area Under the Curve Receiver Operating Characteristic (AUCROC), which is a qualitative indicator for the binary classification ranging from 0 to 1 with 0.5 indicating a classification not better than random guessing.

III. Results

A. Statistical Analysis

A univariate statistical analysis was carried out on both demographic and clinical variables and on the kinematic and kinetic parameters, separately. However, this analysis was initially carried out on the complete dataset (comprising 90 patients). Subsequently, in order to demonstrate that differences in kinematic and kinetic variables were not dependent on age but rather on the patients' pathological condition, a statistical analysis was conducted on a reduced dataset (comprising 47 patients) matched for age (Table I).

From the analysis on the complete dataset, the two groups differed for age ($p = 0.003$), H&Y scores ($p = 0.033$), MDS-UPDRS-Part III ($p = 0.039$) and, consequently, showed a trend toward significance on total MDS-UPDRS ($p = 0.078$) (Table I). The same significances among clinical and

TABLE I
COMPARISON OF DEMOGRAPHIC AND CLINICAL FEATURES BETWEEN PD-MCI AND PD-NOMCI THROUGH A UNIVARIATE STATISTICAL ANALYSIS (MEAN ± STANDARD DEVIATION) ON BOTH COMPLETE AND AGE-MATCHED DATASET. SIGNIFICANT P-VALUES ARE HIGHLIGHTED IN BOLD. SIGNIFICANCE LEVEL AT 0.05

Variables	Complete Dataset			Sub Dataset		
	PD-noMCI (n=50)	PD-MCI (n=40)	p-value	PD-noMCI (n=23)	PD-MCI (n=24)	p-value
Age (years)	61,35 ± 8,11	67,02 ± 9,03	**0,003**	65,59 ± 3,95	65,35 ± 4,63	0,741
BMI	26,72 ± 3,03	28,25 ± 3,92	**0,027**	26,33 ± 2,95	28,87 ± 3,55	**0,015**
Disease Duration (years)	4,40 ± 2,60	4,94 ± 2,41	0,221	4,37 ± 2,79	4,98 ± 2,46	0,321
Hoehn & Yahr	1,79 ± 0,40	1,95 ± 0,32	**0,033**	1,69 ± 0,42	1,97 ± 0,31	**0,012**
LEDD (mg)	382,41 ± 233,46	457,31 ± 236,41	0,325	303,19 ± 180,14	392,20 ± 158,13	0,530
MDS-UPDRS-Part I	6,96 ± 4,10	9,53 ± 7,27	0,159	6,57 ± 3,61	10,38 ± 7,85	0,091
MDS-UPDRS-Part II	8,20 ± 5,80	8,52 ± 5,47	0,490	8,20 ± 5,63	8,54 ± 5,30	0,353
MDS-UPDRS-Part III	22,43 ± 10,05	24,68 ± 8,02	**0,039**	22,43 ± 10,46	24,58 ± 7,29	**0,036**
MDS-UPDRS-Part IV	1,92 ± 3,02	1,40 ± 2,66	0,315	1,74 ± 2,59	0,67 ± 1,52	0,127
Total MDS-UPDRS	39,51 ± 17,11	44,13 ± 17,48	0,078	37,78 ± 17,35	44,17 ± 16,91	0,062

PD, Parkinson's Disease; MCI, Mild Cognitive Impairment; BMI, Body Mass Index; LEDD, Levodopa Equivalent Daily Dose; MDS-UPDRS, Movement Disorder Society Unified Parkinson's Disease Rating Scale.

demographic variables, except for age, were present in the reduced dataset.

Mean values and standard deviations of kinematic and kinetic features for the three gait trials, showing significant p-values or statistical trends (p-values < 0.1) when comparing PD-MCI and PD-noMCI groups, are reported in table II and III. In the supplementary materials, tables S1 and S2, all p-values for each single variable are shown.

1) Kinematics: The kinematic differences between the study groups were more pronounced on sagittal plane in different angle joints and in all three tasks (GAIT, MOT and COG) as shown in Table II.

PD-MCI patients walked with a markedly increased pelvic flexion on sagittal plane, as displayed by the increase on both antiversum and retroversum pelvic tilt (p=0.016/p= 0.018 in GAIT, p=0.027/p=0.009 in MOT and p=0.011/p=0.012 in the COG task, respectively). In addition, pelvic tilt ROM was significantly increased for PD-MCI in the GAIT task (p=0.024).

Likewise, PD-MCI patients showed increased hip flexion during the whole cycle and reduced hip extension during stance phase. In particular, the hip flexion was significantly increased in GAIT and MOT tasks at initial contact (p=0.007, p=0.044, respectively) as well as in all three tasks (p=0.006, p=0.014, p=0.053, respectively) during swing phase, while hip extension in stance phase was significantly reduced (p=0.002, p=0.022, p=0.004, respectively). Moreover, on the transversal plane, the hip internal-external rotation ROM was increased in all gait tasks with statistical differences in the GAIT task (p=0.018) and statistical trend in dual-tasks (p=0.087 in MOT and p=0.074 in COG, respectively), thus indicating that PD-MCI tend to increment hip internal-rotation.

Similarly, PD-MCI patients showed a marked increase of knee flexion at initial contact in gait conditions other than COG task (p=0.047 in GAIT, p=0.039 in MOT tasks, respectively) in combination with reduced knee extension in mid-stance in GAIT, MOT and COG tasks (p=0.009, p=0.002 and p=0.013, respectively) and a reduced knee ROM (p=0.004) in the COG task. When evaluating the knee joint on the transversal plane, PD-MCI showed a reduced value in the maximum of the knee internal-external rotation (p= 0.018, p=0.018 and p=0.043, respectively in GAIT, MOT and COG task), thus indicating that PD-MCI tend to adopt a more pronounced external-rotation as compared with PD-noMCI.

Regarding the ankle joint, although the maximal dorsal flexion did not differ between the groups, PD-MCI patients walked with slightly increased dorsiflexion during the whole stance phase. Moreover, the values of plantarflexion observed in the swing phase differed significantly between the two groups in GAIT and COG tasks (p<0.001 and p=0.016, respectively). In particular, PD-MCI vs PD-noMCI showed increased plantarflexion during GAIT task but reverted this pattern toward reduced plantarflexion during COG task. Although there was no significant difference in ankle plantarflexion in the MOT task (p=0.088), its mean values differed between the two groups following the pattern displayed during COG task.

Finally, PD-MCI vs PD-noMCI displayed significant reduced pelvic obliquity on the frontal plane during COG task and reduced trunk rotation on the transversal plane during both MOT and COG tasks. Apart from those reported above, other kinematics measures did not differ between the two groups. The results from the analysis on the reduced dataset confirm the goodness of the findings from the overall population regarding the kinematic variables.

2) Kinetics: The kinetic differences between PD-MCI and PD-noMCI patients were observed in the GAIT and COG tasks, as shown in Table III. In the hip joint, hip extension moment was reduced in PD-MCI compared with PD-noMCI (p=0.041, p=0.044 in GAIT and COG task, respectively). Likewise, PD-MCI vs PD-noMCI showed reduced hip power generated (p=0.029, p = 0.004 in GAIT and COG task, respectively) and decreased power absorbed (p=0.016 in the GAIT task) in the stance phase. Moreover, PD-MCI showed reduction of the hip flexion moment both in single and dual-task even if it did not differ between the groups. In addition, during the COG task, PD-MCI vs PD-noMCI showed reduced knee extension moment (p<0.001) and decreased knee power absorbed (p=0.011), whereas, at the ankle joint, they displayed an increase of moment at loading response (p=0.002), in combination with a reduction in power generated (p=0.016)

TABLE II

UNIVARIATE STATISTICAL ANALYSIS OF SIGNIFICANT KINEMATIC PARAMETERS OF GAIT, MOT AND COG TASK (MEAN ± STANDARD DEVIATION) ON BOTH COMPLETE AND AGE-MATCHED DATASET. SIGNIFICANT P-VALUES ARE HIGHLIGHTED IN BOLD. SIGNIFICANCE LEVEL AT 0,05

JOINT	KINEMATIC PARAMETER (°)	Complete Dataset			Sub-Dataset		
		PD-noMCI (n=50)	PD-MCI (n=40)	p-value	PD-noMCI (n=23)	PD-MCI (n=24)	p-value
GAIT							
Pelvis	**Antiversum Tilt**	6,84 ± 6,19	10,69 ± 7,66	**0,016**	7,82±3,90	12,58±6,10	**0,014**
	Retroversum Tilt	4,05 ± 6,32	7,78 ± 7,41	**0,018**	6,20±3,80	10,14±5,54	**0,043**
	ROM Tilt	2,79 ± 0,89	2,92 ± 1,17	**0,024**	1,62±0,10	2,44±0,56	**0,068**
Trunk	**Internal Rotation**	3,25 ± 1,10	2,87 ± 0,87	0,083	3,25 ± 0,72	3,19 ± 0,95	0,495
	High Obliquity	1,44 ± 0,72	1,69 ± 0,76	0,055	1,52 ± 0,79	1,84 ± 0,74	0,075
	Low Obliquity	-1,44 ± 0,77	-1,69 ± 0,79	0,072	-1,53 ± 0,83	-1,80 ± 0,75	0,082
	ROM Obliquity	2,88 ± 1,49	3,38 ± 1,53	0,055	3,05 ± 1,62	3,64 ± 1,47	0,065
Hip	**ROM Rotation**	13,94 ± 3,34	16,23 ± 4,34	**0,018**	13,66±3,91	17,03±1,79	**0,006**
	Flexion	28,65 ± 8,46	34,56 ± 9,80	**0,006**	26,27±8,98	36,22±10,32	**0,011**
	Extension	-12,68 ± 9,36	-5,16 ± 11,30	**0,002**	-16,95±9,66	-3,40±12,44	**0,020**
	CI Flexion	26,96 ± 8,18	32,62 ± 9,84	**0,007**	24,51±8,98	34,77±10,32	**0,042**
Knee	**Internal Rotation**	-0,50 ± 11,94	-1,44 ± 6,95	**0,018**	2,41 ± 14,25	-1,75 ± 5,01	**0,035**
	CI Flexion	8,45 ± 5,56	11,00 ± 5,36	**0,047**	7,32±3,91	10,18±4,67	0,071
	Extension	2,15 ± 6,09	5,93 ± 6,13	**0,009**	1,16±5,78	5,49±5,81	**0,029**
	ROM Flex-Extension	54,11 ± 5,14	51,90 ± 6,44	0,096	55,31±0,82	51,93±0,02	**0,037**
Ankle	**External Rotation**	-21,63 ± 5,07	-19,66 ± 6,74	**0,049**	-21,22 ± 4,95	-18,94 ± 3,89	**0,047**
	Plantarflexion	-14,71 ± 5,50	-22,21 ± 8,13	**<0,001**	-15,21±5,66	--22,01±7,79	**0,041**
	ROM Dors-Plantarflexion	26,37 ± 4,78	34,53 ± 8,00	**<0,001**	26,21±4,25	33,54±8,10	**0,005**
MOT							
Pelvis	**Antiversum Tilt**	6,82 ± 6,13	10,24 ± 7,79	**0,027**	5,79 ± 7,34	10,40 ± 8,23	**0,047**
	Retroversum Tilt	3,32 ± 6,44	7,43 ± 7,60	**0,009**	1,24±2,73	8,16±3,31	**0,032**
Trunk	**Internal Rotation**	3,20 ± 1,11	2,61 ± 0,88	**0,008**	3,10 ± 1,08	2,81 ± 0,87	0,087
	External Rotation	-3,12 ± 1,13	-2,70 ± 0,97	0,054	-3,02 ± 1,11	-2,86 ± 0,84	0,062
	ROM Rotation	6,33 ± 2,23	5,31 ± 1,80	**0,025**	6,12 ± 2,18	5,68 ± 1,67	**0,042**
Hip	**ROM Rotation**	14,97 ± 4,38	17,34 ± 6,45	0,087	15,57 ± 4,52	17,93 ± 6,54	0,074
	Flexion	28,51 ± 8,86	34,18 ± 11,24	**0,014**	26,02±10,12	37,72±12,16	**0,046**
	Extension	-11,31 ± 10,06	-5,01 ± 13,85	**0,022**	-16,33±10,05	-2,53±11,93	**0,004**
	CI Flexion	26,67 ± 8,56	31,34 ± 11,65	**0,044**	23,85±9,47	35,49±10,88	**0,020**
Knee	**Internal Rotation**	-0,20 ± 11,55	-0,33 ± 6,78	**0,018**	1,73 ± 13,85	-0,60 ± 5,41	**0,049**
	CI Flexion	8,59 ± 6,37	10,81 ± 7,42	**0,039**	6,05±4,68	10,83±5,81	**0,037**
	Extension	2,43 ± 5,91	6,93 ± 6,61	**0,002**	1,18±5,92	6,40±6,11	**0,013**
Ankle	**External Rotation**	-20,65 ± 5,42	-20,59 ± 7,04	0,086	-21,56 ± 6,62	-19,43 ± 3,91	0,076
	ROM Rotation	13,55 ± 3,26	11,56 ± 4,23	**0,026**	12,41± 2,30	11,96 ± 2,97	**0,045**
	Dorsiflexion	12,03 ± 3,60	13,56 ± 3,71	0,063	11,20 ± 3,64	12,84 ± 3,63	0,072
	Plantarflexion	-14,77 ± 9,15	-11,90 ± 5,68	0,088	-13,79 ± 4,35	-13,31± 4,79	0,098
COG							
Pelvis	**Antiversum Tilt**	7,05 ± 6,29	10,99 ± 7,71	**0,011**	5,22±3,68	11,21±2,55	**0,050**
	Retroversum Tilt	4,01 ± 6,31	7,86 ± 7,57	**0,012**	2,32±3,29	8,44±2,52	**0,045**
	Low Obliquity	-2,37 ± 1,08	-2,02 ± 1,30	**0,040**	-2,33 ± 1,37	-1,77 ± 0,92	0,077
	ROM Obliquity	4,73 ± 2,12	4,14 ± 2,44	0,097	2,59±1,36	3,48±1,92	0,070
Trunk	**External Rotation**	-3,61 ± 1,16	-3,12 ± 1,18	**0,029**	-3,53 ± 1,14	-3,17 ± 1,06	**0,039**
	ROM Rotation	6,98 ± 2,37	6,18 ± 2,43	0,063	6,74 ± 2,28	6,33 ± 2,19	0,083
Hip	**ROM Rotation**	13,71 ± 3,89	15,45 ± 4,34	0,074	13,25 ± 2,68	16,13 ± 5,18	0,064
	Flexion	27,77 ± 8,89	32,10 ± 10,38	0,053	24,25 ± 9,22	36,28 ± 9,30	**0,041**
	Extension	-11,74 ±9,77	-3,91 ± 13,21	**0,004**	-15,97 ± 0,07	-1,34 ± 11,54	**0,009**
	ROM Flex-Extension	39,50 ± 5,63	36,01 ± 6,77	**0,021**	40,21 ± 3,94	37,62 ± 5,91	**0,009**
	CI Flexion	26,08 ± 8,74	29,83 ± 10,66	0,078	22,45 ± 9,29	34,17 ± 9,76	**0,041**
Knee	**Internal Rotation**	-1,59 ± 10,47	-3,02 ± 7,79	**0,043**	-2,24 ± 7,56	-3,14 ± 5,68	0,066
	Extension	2,16 ± 6,30	6,21 ± 7,64	**0,013**	1,24 ± 4,75	5,86 ± 6,38	**0,020**
	ROM Flex-Extension	52,09 ± 5,64	47,64 ± 7,49	**0,004**	52,55 ± 5,85	49,66 ± 5,88	**0,042**
Ankle	**External Rotation**	-22,73 ± 5,35	-20,77 ± 7,20	**0,045**	-22,19 ± 7,03	-20,73 ± 4,59	0,062
	ROM Rotation	12,07 ± 5,51	10,24 ± 4,04	0,087	12,24 ± 7,85	10,75 ± 3,26	0,076
	Dorsiflexion	11,11 ± 3,76	12,66 ± 3,74	**0,049**	10,24 ± 3,55	11,74 ± 3,85	0,052
	Plantarflexion	-13,42 ± 5,47	-10,32 ± 5,89	**0,016**	-12,64 ± 4,03	-10,94 ± 4,89	**0,032**

ROM, Range of Motion; CI, Initial Contact.

and an increase in power absorbed (p=0.009). The results from the analysis on the reduced dataset confirm the goodness of the findings from the overall population regarding the kinetic variables.

TABLE III
UNIVARIATE STATISTICAL ANALYSIS OF SIGNIFICANT KINETIC PARAMETERS OF GAIT, MOT AND COG TASK (MEAN ± STANDARD DEVIATION) ON BOTH TOTAL AND AGE-MATCHED DATASET. SIGNIFICANT P-VALUES ARE HIGHLIGHTED IN BOLD. SIGNIFICANCE LEVEL AT 0.05

JOINT	KINETIC PARAMETER (u.m.)	Complete Dataset			Sub-Dataset		
		PD-noMCI (n=50)	PD-MCI (n=40)	p-value	PD-noMCI (n=23)	PD-MCI (n=24)	p-value
GAIT							
Hip	**Extension moment in stance phase (N*m/Kg)**	0,78 ± 0,29	0,65± 0,24	**0,041**	0,88 ± 0,24	0,84± 0,41	0,833
	Power generated in stance (W/Kg)	1,04 ± 1,02	0,78 ± 0,28	**0,029**	0,80 ± 0,38	0,76 ± 0,27	0,545
	Power absorbed in stance (W/Kg)	-0,93 ± 0,47	-0,69 ± 0,38	**0,016**	-0,88 ± 0,35	-0,47± 0,29	**0,001**
COG							
Hip	**Extension moment in stance phase (N*m/Kg)**	0,63 ± 0,22	0,54 ± 0,19	**0,044**	0,62 ± 0,14	0,43± 0,18	**0,002**
	Flexion moment in stance phase (N*m/Kg)	-0,70 ± 0,40	-0,56 ± 0,37	0,093	-0,89 ± 0,29	-0,72 ± 0,32	**0,045**
	Power generated in stance (W/Kg)	0,94 ± 0,54	0,65 ± 0,27	**0,004**	0,73 ± 0,23	0,50 ± 0,19	**0,001**
Knee	**Extension moment in stance phase (N*m/Kg)**	0,49 ± 0,23	0,28 ± 0,16	**<0,001**	0,52 ± 0,19	0,40 ± 0,13	**0,046**
	Flexion moment in stance phase (N*m/Kg)	-0,32 ± 0,19	-0,26 ± 0,16	0,078	-0,36 ± 0,16	-0,30 ± 0,16	0,172
	Power absorbed in stance (W/Kg)	-0,89 ± 0,46	-0,49 ± 0,20	**0,011**	-0,81 ± 0,31	-0,46 ± 0,20	**0,001**
Ankle	**Moment at loading response (N*m/Kg)**	0,05 ± 0,09	0,13 ± 0,14	**0,002**	0,09 ± 0,01	0,12 ± 0,11	**0,101**
	Power generated in stance (W/Kg)	2,09 ± 1,08	1,87 ± 0,60	**0,016**	2,45 ± 0,78	1,80 ± 0,56	**0,019**
	Power absorbed in stance (W/Kg)	-0,23 ± 0,15	-0,33 ± 0,28	**0,009**	-0,19± 0,15	-0,31 ± 0,14	**0,001**

GRF, Ground Reaction Force.

B. Classification

Subsequently, kinematic and kinetic parameters of each gait task (GAIT, MOT and COG) were used to build the ML classifiers, separately. Table IV shows the evaluation metrics of the ML algorithms for the three gait trials. In the supplementary materials, Table S3 shows all evaluation metrics for each classifier.

1) Kinematics: In the GAIT task, almost all the classifiers reached an accuracy over than 80% on kinematic parameters. Particularly, different tree-based methods achieved an accuracy greater than 85%. Indeed, GBT obtained the best accuracy (87.1%), followed by DT (86.1%), SVM (83.1%). In terms of other evaluation metrics, GBT and SVM showed the highest AUCROC (0.871 and 0.831, respectively). However, GBT showed low power in the identification of presence and absence of MCI (Se = 66.7%, Sp=66.7% and Pr=57.1%, respectively), whereas SVM showed a good trade-off among these evaluation metrics with the best capability to detect the patients belonging to the group with and without MCI (Se = 85.7%, Sp=81.8% and Pr=75.0%). As concern DT, although it showed an accuracy over than 80%, its capability to identify the affected group was only around 65%. Among the best classifiers, RF also reached good performance with values over the 80% for the AUCROC (0.815), specificity (88.9%) and precision (81.8%) and around the 75% for the accuracy (75.2%) and sensitivity (75.0%).

In contrast to GAIT task, the performance of the ML classifiers was severely reduced in the dual tasks [65].

In the MOT task, LDA classifier showed higher accuracy (71.3%) and a good ability to identify the true negative (sp = 75.5%). The DT and GBT algorithms confirmed their capability to classify the two groups with an accuracy and an AUCROC over than 60%.

In the COG task, RF, DT and KNN reached accuracy values over 60% (62.9%, 61.8% and 61.8%, respectively) and AUCROC values in the range between 60% and 70%.

In dual-task experiments, the best performance by the classifiers was reached in the classification of patients without MCI. Indeed, different algorithms, such as SVM, KNN, LDA and DT, achieved over 70% specificity, while different other algorithms showed lower sensitivity with values under the 60% in the MOT task and under 50% in the COG task (Table S3).

2) Kinetics: With regards to the kinetic parameters, the best results were obtained in the COG dual task (Table IV). Trees-based algorithms showed the best performance in the classification of PD-MCI and PD-noMCI patients. Indeed, DT, RF and BGT reached an accuracy greater than 75% (76.9%, 77.5% and 76.4%, respectively) and an AUCROC over than 85% for the ensemble methods (0.850 and 0.857). In addition, RF and GBT obtained the highest specificity and precision with metric values greater than 80% (RF: 89.8% and GBT: 80.0%).

In contrast to COG task, the accuracies obtained by ML classifiers on kinetic parameters were around 60% in GAIT and 70% in the MOT task. Nevertheless, DT and GBT achieved the best evaluation metrics. In the GAIT task,

TABLE IV
EVALUATION METRICS OF THE BEST CLASSIFIERS ON KINEMATIC AND KINETIC PARAMETERS FOR EACH TASK

KINEMATICS					
GAIT					
Classifiers	**AUCROC**	**Ac [%]**	**Se [%]**	**Sp [%]**	**Pr [%]**
DT	0.670	86,1	66,7	72,2	75,0
RF	0.815	75,2	75,0	88,9	81,8
GBT	0.871	87,1	66,7	66,7	57,1
SVM	0.831	83,1	85,7	81,8	75,0
MOT					
Classifiers	**AUCROC**	**Ac [%]**	**Se [%]**	**Sp [%]**	**Pr [%]**
DT	0.674	67,1	60,0	73,4	64,8
GBT	0.606	62,8	60,0	61,2	55,8
LDA	0.595	71,3	40,0	75,5	57,1
COG					
DT	0.650	61,8	47,5	73,4	59,3
RF	0.634	62,9	55,0	69,3	59,4
k-NN	0.702	61,8	40,0	79,5	61,5
KINETICS					
GAIT					
Classifiers	**AUCROC**	**Ac [%]**	**Se [%]**	**Sp [%]**	**Pr [%]**
DT	0,723	69,7	63,3	77,5	77,5
GBT	0,702	63,3	65,3	67,5	71,1
SVM	0,600	62,8	65,0	73,8	65,0
MOT					
Classifiers	**AUCROC**	**Ac [%]**	**Se [%]**	**Sp [%]**	**Pr [%]**
DT	0,780	70,8	67,5	73,5	73,5
GBT	0,781	75,3	77,6	72,5	77,6
COG					
Classifiers	**AUCROC**	**Ac [%]**	**Se [%]**	**Sp [%]**	**Pr [%]**
DT	0,726	76,9	62,5	75,5	66,7
RF	0,850	77,5	62,5	89,8	83,3
GBT	0,857	76,4	73,5	80,0	81,8

DT = Decision Tree; RF=Random Forest; GBT= Gradient Boosted Tree; SVM= Support Vector Machine; LDA = Linear Discriminant Analysis; k-NN=k-NumNeighbors; AUCROC =Area Under ROC Curve; Ac= Accuracy; Se = Sensitivity; Sp = Specificity; Pr = Precision; GAIT = Single walking task; MOT = Motor dual-task; COG = Cognitive dual-task.

DT showed the highest values in all metrics (AUCROC = 0,723; Ac = 69.7%; Sp = 63.3%; se = 77.5%; Pr = 77.5%) followed by GBT (Ac = 63.3%; AUCROC = 0.702). In the MOT task, both tree-based classifiers reached values greater than 70% in accuracy and AUCROC.

C. Feature Selection

All kinematic and kinetic gait features selected by wrapper method and performance metrics according to this classification on reduced subsets are summarized in Table V. In Table S4 of the supplementary material the evaluation metrics and features selected by all classifiers are shown.

In agreement with the previous classification on the whole kinematic dataset, the major number of kinematic parameters belonged to GAIT and COG task. Table V shows that most of gait features helping in classifying PD-MCI and PD-noMCI patients are related to the ankle joint movements on sagittal plane, and, to a lesser extent, to trunk and pelvis movements on transversal and frontal plane, as shown in Table IV and Table S4.

Among the tested classification algorithms, DT reached an accuracy (83.3%) as well as AUCROC (0.856) (greater than 80%), using the lowest number of features selected (n° = 2). This was followed by KNN with scores around 80% (Ac=81.5% and AUCROC=0.817). Moreover, NB. RF, GBT and LDA classified the two groups with an accuracy around 70% (77.8%, 72.2%, 71.9% and 73.0%, respectively). Conversely, SVM selected the highest number of features (n° = 5) and showed the lowest result in terms of accuracy (67.4%).

Similar to the kinematics analysis, the number of kinetic attributes employed for each tested algorithm is shown in Table V and Table S4. Most gait features capable of classifying the groups are related to hip power generated and hip moment extension, knee power absorbed and knee moment extension in the COG task. Additionally, we identified knee moment extension in the GAIT task and hip power generated and absorbed in the MOT task.

With regards to classification, KNN obtained the highest accuracy (79.8%), precision (79.0%) and specificity (83.7%), while exploiting the lowest number of kinematic features (n° = 3). This is followed by tree-based classifiers RF and GBT which reached an accuracy over 75% and an AUCROC over 85% using 8 and 5 features selected, respectively. Conversely, the NB algorithm got the lowest accuracy (70.8%) and precision (66.7%).

IV. DISCUSSION

In the present study, we show that the presence of MCI in PD patients is coupled with kinematic and kinetic modifications of gait cycle that can identify two different phenotypes of the disease. Indeed, as displayed by the

TABLE V
FEATURES SELECTED AND EVALUATION METRICS OF THE BEST CLASSIFIERS ON KINEMATIC AND KINETIC PARAMETERS BY WRAPPER METHOD

KINEMATICS							
Classifiers	**AUCROC**	**Ac [%]**	**Se [%]**	**Sp [%]**	**Pr [%]**	**N° Features**	**Features**
DT	0.856	83,3%	75,0%	90,0%	85,7%	2	GAIT Ankle Extension COG Pelvis Low Obliquity
k-NN	0.817	81,5%	80,0%	83,3%	76,9%	3	GAIT Pelvic High Obliquity COG Ankle CI Flexion COG Ankle Flexion
KINETICS							
Classifiers	**AUCROC**	**Ac [%]**	**Se [%]**	**Sp [%]**	**Pr [%]**	**N° Features**	**Features**
RF	0.854	74,2%	70,0%	77,6%	71,8%	3	COG Hip Max Generated Power MOT Knee Flexion Moment GAIT Vertical GRF
GBT	0.863	74,1%	75,0%	73,5%	69,8%	5	COG Vertical GRF COG Knee Extension Moment COG Hip Extension Moment COG Hip Flexion Moment MOT Hip Max Absorbed Power
k-NN	0.848	79,8%	75,0%	83,7%	78,9%	3	COG Vertical GRF COG Hip Max Generated Power MOT Knee Moment of max flexion

DT = Decision Tree; RF=Random Forest; GBT= Gradient Boosted Tree; k-NN=k-NumNeighbors; AUCROC =Area Under ROC Curve; Ac= Accuracy; Se = Sensitivity; Sp = Specificity; Pr = Precision; GAIT = Single walking task; MOT = Motor dual-task; COG = Cognitive dual-task; GRF = Ground Reaction Force.

demographical and clinical comparison between the two groups, PD-MCI patients were older and more impaired, in accordance with published data [7], while showing comparable disease duration and LEDD. Such differences mirror two of the main clinical features associated with MCI in PD, suggesting a close relationship among MCI, age and more severe motor impairment. In other terms, gait features observed in PD-MCI patients reflect the contribution of all these factors, that are inseparable in real-life clinical settings. Anyway, in order to minimize the possible confounding role of age, we have performed an additional sub-group analysis on age-matched PD-MCI and PD-noMCI patients. The sub-analysis showed that the findings remained significant, thus further supporting the reliability of our results.

Regarding kinematic analysis, PD-MCI as compared with PD-noMCI, showed increased sagittal flexion in the pelvis, hip and knee in all three tasks, suggesting that such features may represent the expression of a more malignant phenotype in which cognitive dysfunction coexists with more severe axial symptoms [66]. In addition, they showed increased internal-rotation at the pelvis and augmented external-rotation at the knee that may be interpreted as compensations for the abnormal postural flexion [67].

When assessing ankle kinematics, PD-MCI as compared to PD-noMCI showed increased plantarflexion during GAIT task and the reversion of this pattern, i.e. reduced plantarflexion, in the dual task condition. Augmented plantarflexion may constitute the compensation for both the excessive knee flexion and the decreased demand on proximal joints, due to the reduction of the physiological age-related distal-to-proximal shift in joint kinetics in PD patients [68], [69], [70]. Under dual task conditions, PD-MCI tended to reduce such compensation, thus increasing heel rocker with increased instability [67]. Accordingly, reduced pelvic obliquity and trunk rotation under dual task conditions would represent the response to the decreased ankle plantarflexion [67].

With regards to the kinetic analysis, PD-MCI vs PD-noMCI displayed reductions in both moment (dynamic force) and power (velocity of dynamic force) at the hip joint in both GAIT and COG task, whereas, only during COG task, they showed reduction in both moment and power at the knee joint with corresponding increased moment, reduced energy generation and augmented energy absorption at the ankle joint. On the one hand, these findings suggest that the lack of physiological age-related distal-to-proximal shift in joint kinetics in PD patients [70] is more evident in the PD phenotype associated with cognitive dysfunction; on the other hand they imply that PD-MCI show reduced control at the ankle joint, as suggested by increased energy absorption [71], especially under dual-task conditions.

When analyzing ML classifications based on kinematic variables, our findings suggest that kinematic patterns distinguishing PD-MCI from PD-noMCI mainly loaded on GAIT task rather than on dual-task features, mirroring, as reported above, a more malignant phenotype, independently from cognitive contribution to such features. On the contrary, when examining ML classification based on kinetic parameters, our results suggest that the most accurate algorithms able to differentiate PD-MCI from PD-noMCI loaded on COG task variables. Dual-task interference tasks engage shared

higher-order neural networks which are involved in the simultaneous performance of gait and the concomitant task [28], [72]; therefore, these findings might indicate a peculiar cortical contribution on joint forces scaling in PD patients. Certainly, further studies are needed to confirm these hypotheses.

The present study has some limitations. In the first instance, in the present study we did not include an age-matched healthy control group. This might have better pointed identified differences due to PD without MCI, along with those associated with PD-MCI. A direct comparison with a healthy control group was beyond the scope of the present study. In addition, we acknowledge that some results should be regarded as preliminary, and a further validation may be useful. Finally, due to paucity of published data on kinematic and kinetic features in PD patients with cognitive impairment, most interpretations of our novel findings are speculative and hypothetical at this stage and need further confirmation.

V. Conclusion

In conclusion, our findings suggest two main features that may have an impact on both PD pathophysiological knowledge and rehabilitation therapy approach. First, most kinematic features distinguishing PD-MCI from PD-noMCI identify a worse disease phenotype in which cognitive impairment coexists with more severe posture and gait dysfunction. Second, kinetic findings might suggest that some cortical areas shared with cognitive processes may have a specific role on force scaling in PD.

References

[1] M. J. Armstrong and M. S. Okun, "Diagnosis and treatment of Parkinson disease: A review," *Jama*, vol. 323, no. 6, pp. 548–560, Feb. 2020.

[2] H. Takahashi and K. Wakabayashi, "The cellular pathology of Parkinson's disease," *Neuropathology*, vol. 21, no. 4, pp. 315–322, Dec. 2001, doi: 10.1046/j.1440-1789.2001.00403.x.

[3] K. Kieburtz and K. B. Wunderle, "Parkinson's disease: Evidence for environmental risk factors," *Movement Disorders*, vol. 28, no. 1, pp. 8–13, Jan. 2013, doi: 10.1002/mds.25150.

[4] S. Sveinbjornsdottir, "The clinical symptoms of Parkinson's disease," *J. Neurochem.*, vol. 139, pp. 318–324, Oct. 2016.

[5] W. Poewe, "Non-motor symptoms in Parkinson's disease," *Eur. J. Neurol.*, vol. 15, no. s1, pp. 14–20, Apr. 2008, doi: 10.1111/j.1468-1331.2008.02056.x.

[6] K. R. Chaudhuri, D. G. Healy, and A. H. V. Schapira, "Non-motor symptoms of Parkinson's disease: Diagnosis and management," *Lancet Neurol*, vol. 5, no. 3, pp. 235–245, Mar. 2006, doi: 10.1016/S1474-4422.

[7] C. Baiano, P. Barone, L. Trojano, and G. Santangelo, "Prevalence and clinical aspects of mild cognitive impairment in Parkinson's disease: A meta-analysis," *Movement Disorders*, vol. 35, no. 1, pp. 45–54, Jan. 2020, doi: 10.1002/mds.27902.

[8] D. Aarsland et al., "Cognitive decline in Parkinson disease," *Nature Rev. Neurol.*, vol. 13, no. 4, pp. 217–231, Apr. 2017, doi: 10.1038/nrneurol.2017.27.

[9] D. Aarsland et al., "Parkinson disease-associated cognitive impairment," *Nature Rev. Disease Primers*, vol. 7, no. 1, pp. 1–23, Jul. 2021, doi: 10.1038/s41572-021-00280-3.

[10] P. Barone, D. Aarsland, D. Burn, M. Emre, J. Kulisevsky, and D. Weintraub, "Cognitive impairment in nondemented Parkinson's disease," *Movement Disorders*, vol. 26, no. 14, pp. 2483–2495, Dec. 2011, doi: 10.1002/mds.23919.

[11] I. Litvan et al., "Diagnostic criteria for mild cognitive impairment in Parkinson's disease: Movement disorder society task force guidelines," *Movement Disorders*, vol. 27, no. 3, pp. 349–356, Mar. 2012.

[12] D. Muslimovic, B. Post, J. D. Speelman, and B. Schmand, "Cognitive profile of patients with newly diagnosed Parkinson disease," *Neurology*, vol. 65, no. 8, pp. 1239–1245, Oct. 2005, doi: 10.1212/01.wnl.0000180516.69442.95.

[13] G. Santangelo et al., "Mild cognitive impairment in newly diagnosed Parkinson's disease: A longitudinal prospective study," *Parkinsonism Rel. Disorders*, vol. 21, no. 10, pp. 1219–1226, Oct. 2015, doi: 10.1016/j.parkreldis.2015.08.024.

[14] R. Baker, A. Esquenazi, M. G. Benedetti, and K. Desloovere, "Gait analysis: Clinical facts," *Eur. J. Phys. Rehabil. Med.*, vol. 52, pp. 560–574, Jul. 2016.

[15] R. Baker, "Gait analysis methods in rehabilitation," *J. NeuroEngineering Rehabil.*, vol. 3, no. 1, p. 4, Mar. 2006, doi: 10.1186/1743-0003-3-4.

[16] G. Cicirelli, D. Impedovo, V. Dentamaro, R. Marani, G. Pirlo, and T. R. D'Orazio, "Human gait analysis in neurodegenerative diseases: A review," *IEEE J. Biomed. Health Informat.*, vol. 26, no. 1, pp. 229–242, Jan. 2022, doi: 10.1109/JBHI.2021.3092875.

[17] J. Dicharry, "Kinematics and kinetics of gait: From lab to clinic," *Clinics Sports Med.*, vol. 29, no. 3, pp. 347–364, Jul. 2010, doi: 10.1016/j.csm.2010.03.013.

[18] P. De Blasiis et al., "Quantitative evaluation of upright posture by X-ray and 3D stereophotogrammetry with a new marker set protocol in late onset pompe disease," *J. Neuromuscular Diseases*, vol. 8, no. 6, pp. 979–988, Nov. 2021, doi: 10.3233/jnd-210663.

[19] P. De Blasiis et al., "Kinematic evaluation of the sagittal posture during walking in healthy subjects by 3D motion analysis using DB-total protocol," *J. Funct. Morphology Kinesiol.*, vol. 7, no. 3, p. 57, Aug. 2022, doi: 10.3390/jfmk7030057.

[20] P. De Blasiis et al., "Sagittal kinematics and imbalance of the spine and whole body during walking in late-onset pompe disease," *J. Neurophysiology*, vol. 130, no. 2, pp. 353–363, Aug. 2023, doi: 10.1152/jn.00142.2023.

[21] P. Arpaia et al., "Executive functions assessment based on wireless EEG and 3D gait analysis during dual-task: A feasibility study," *IEEE J. Translational Eng. Health Med.*, vol. 12, pp. 268–278, 2024, doi: 10.1109/JTEHM.2024.3357287.

[22] P. Arpaia et al., "Electroencephalographic-based wearable instrumentation to monitor the executive functions during gait: A feasibility study," *Acta IMEKO*, vol. 12, no. 2, pp. 1–6, May 2023, doi: 10.21014/actaimeko.v12i2.1460.

[23] L. D. Biase et al., "Quantitative analysis of bradykinesia and rigidity in Parkinson's disease," *Frontiers Neurol.*, vol. 9, no. 1, pp. 1–7, 2018.

[24] S. Summa et al., "Assessing bradykinesia in Parkinson's disease using gyroscope signals," in *Proc. Int. Conf. Rehabil. Robot. (ICORR)*, Jul. 2017, pp. 1556–1561, doi: 10.1109/ICORR.2017.8009469.

[25] M. Amboni et al., "Gait analysis may distinguish progressive supranuclear palsy and Parkinson disease since the earliest stages," *Sci. Rep.*, vol. 11, no. 1, pp. 1–23, Apr. 2021, doi: 10.1038/s41598-021-88877-2.

[26] M. Picillo et al., "Gait analysis in progressive supranuclear palsy phenotypes," *Frontiers Neurol.*, vol. 12, Jun. 2021, Art. no. 674495, doi: 10.3389/fneur.2021.674495.

[27] G. Yogev-Seligmann, J. M. Hausdorff, and N. Giladi, "The role of executive function and attention in gait," *Movement Disorders*, vol. 23, no. 2, pp. 329–342, Feb. 2008.

[28] M. Amboni, P. Barone, and J. M. Hausdorff, "Cognitive contributions to gait and falls: Evidence and implications," *Movement Disorders*, vol. 28, no. 11, pp. 1520–1533, Sep. 2013, doi: 10.1002/mds.25674.

[29] M. Amboni et al., "Gait patterns in parkinsonian patients with or without mild cognitive impairment," *Movement Disorders*, vol. 27, no. 12, pp. 1536–1543, Oct. 2012, doi: 10.1002/mds.25165.

[30] R. Morris, S. Lord, J. Bunce, D. Burn, and L. Rochester, "Gait and cognition: Mapping the global and discrete relationships in ageing and neurodegenerative disease," *Neurosci. Biobehavioral Rev.*, vol. 64, pp. 326–345, May 2016, doi: 10.1016/j.neubiorev.2016.02.012.

[31] L. Bahureksa et al., "The impact of mild cognitive impairment on gait and balance: A systematic review and meta-analysis of studies using instrumented assessment," *Gerontology*, vol. 63, no. 1, pp. 67–83, 2017, doi: 10.1159/000445831.

[32] M. Amboni et al., "Mild cognitive impairment subtypes are associated with peculiar gait patterns in Parkinson's disease," *Frontiers Aging Neurosci.*, vol. 14, Mar. 2022, Art. no. 781480, doi: 10.3389/fnagi.2022.781480.

[33] R. Bouça-Machado et al., "Gait kinematic parameters in Parkinson's disease: A systematic review," *J. Parkinson's Disease*, vol. 10, no. 3, pp. 843–853, Jul. 2020, doi: 10.3233/jpd-201969.

[34] M. E. Morris, J. McGinley, F. Huxham, J. Collier, and R. Iansek, "Constraints on the kinetic, kinematic and spatiotemporal parameters of gait in Parkinson's disease," *Hum. Movement Sci.*, vol. 18, nos. 2–3, pp. 461–483, Jun. 1999, doi: 10.1016/s0167-9457(99)00020-2.

[35] G. N. Lewis, "Stride length regulation in Parkinson's disease: The use of extrinsic, visual cues," *Brain*, vol. 123, no. 10, pp. 2077–2090, Oct. 2000, doi: 10.1093/brain/123.10.2077.

[36] A. Kececi, A. Yildirak, K. Ozyazici, G. Ayluctarhan, O. Agbulut, and I. Zincir, "Implementation of machine learning algorithms for gait recognition," *Eng. Sci. Technol., Int. J.*, vol. 23, no. 4, pp. 931–937, Aug. 2020, doi: 10.1016/j.jestch.2020.01.005.

[37] A. Landolfi et al., "Machine learning approaches in Parkinson's disease," *Current Medicinal Chem.*, vol. 28, no. 32, pp. 6548–6568, Oct. 2021, doi: 10.2174/0929867328999210111211420.

[38] E. Balaji, D. Brindha, and R. Balakrishnan, "Supervised machine learning based gait classification system for early detection and stage classification of Parkinson's disease," *Appl. Soft Comput.*, vol. 94, Sep. 2020, Art. no. 106494, doi: 10.1016/j.asoc.2020.106494.

[39] P.-H. Chen, C.-W. Lien, W.-C. Wu, L.-S. Lee, and J.-S. Shaw, "Gait-based machine learning for classifying patients with different types of mild cognitive impairment," *J. Med. Syst.*, vol. 44, no. 6, p. 107, Apr. 2020, doi: 10.1007/s10916-020-01578-7.

[40] C. Ricciardi et al., "Machine learning can detect the presence of mild cognitive impairment in patients affected by Parkinson's disease," in *Proc. IEEE Int. Symp. Med. Meas. Appl.*, Jun. 2020, pp. 1–6, doi: 10.1109/MeMeA49120.2020.9137301.

[41] M. Russo et al., "Identification of a gait pattern for detecting mild cognitive impairment in Parkinson's disease," *Sensors*, vol. 23, no. 4, p. 1985, Feb. 2023, doi: 10.3390/s23041985.

[42] M. Amboni et al., "Machine learning can predict mild cognitive impairment in Parkinson's disease," *Frontiers Neurol.*, vol. 13, pp. 1–26, Nov. 2022.

[43] M. Martínez, F. Villagra, J. M. Castellote, and M. A. Pastor, "Kinematic and kinetic patterns related to free-walking in Parkinson's disease," *Sensors*, vol. 18, no. 12, p. 4224, Dec. 2018, doi: 10.3390/s18124224.

[44] N. M. Tahir and H. H. Manap, "Parkinson disease gait classification based on machine learning approach," *J. Appl. Sci.*, vol. 12, no. 2, pp. 180–185, Jan. 2012, doi: 10.3923/jas.2012.180.185.

[45] R. B. Postuma et al., "MDS clinical diagnostic criteria for Parkinson's disease," *Movement Disorders*, vol. 30, no. 12, pp. 1591–1601, Oct. 2015, doi: 10.1002/mds.26424.

[46] R. Bhidayasiri and D. Tarsy, "Parkinson's disease: Hoehn and Yahr scale," in *Current Clinical Neurology*. Totowa, NJ, USA: Humana Press, 2012, pp. 4–5.

[47] R. B. Davis, S. Õunpuu, D. Tyburski, and J. R. Gage, "A gait analysis data collection and reduction technique," *Hum. Movement Sci.*, vol. 10, no. 5, pp. 575–587, Oct. 1991, doi: 10.1016/0167-9457(91)90046-z.

[48] M. Amboni et al., "Step length predicts executive dysfunction in Parkinson's disease: A 3-year prospective study," *J. Neurol.*, vol. 265, no. 10, pp. 2211–2220, Oct. 2018, doi: 10.1007/s00415-018-8973-x.

[49] V. E. Kelly, A. J. Eusterbrock, and A. Shumway-Cook, "A review of dual-task walking deficits in people with Parkinson's disease: Motor and cognitive contributions, mechanisms, and clinical implications," *Parkinson's Disease*, vol. 2012, pp. 1–14, Sep. 2012, doi: 10.1155/2012/918719.

[50] O. Huxhold, S.-C. Li, F. Schmiedek, and U. Lindenberger, "Dual-tasking postural control: Aging and the effects of cognitive demand in conjunction with focus of attention," *Brain Res. Bull.*, vol. 69, no. 3, pp. 294–305, Apr. 2006, doi: 10.1016/j.brainresbull.2006.01.002.

[51] A. Gupta, P. Mishra, C. Pandey, U. Singh, C. Sahu, and A. Keshri, "Descriptive statistics and normality tests for statistical data," *Ann. Cardiac Anaesthesia*, vol. 22, no. 1, p. 67, 2019.

[52] M. Russo et al., "Interplay between gait and neuropsychiatric symptoms in Parkinson's disease," *Eur. J. Transl. Myology*, vol. 32, no. 2, pp. 1–28, Jun. 2022, doi: 10.4081/ejtm.2022.10463.

[53] S. Shetty and Y. S. Rao, "SVM based machine learning approach to identify Parkinson's disease using gait analysis," in *Proc. Int. Conf. Inventive Comput. Technol. (ICICT)*, vol. 2, Aug. 2016, pp. 1–5, doi: 10.1109/INVENTIVE.2016.7824836.

[54] D. Trabassi et al., "Machine learning approach to support the detection of Parkinson's disease in IMU-based gait analysis," *Sensors*, vol. 22, no. 10, p. 3700, May 2022, doi: 10.3390/s22103700.

[55] T.-T. Wong, "Performance evaluation of classification algorithms by k-fold and leave-one-out cross validation," *Pattern Recognit.*, vol. 48, no. 9, pp. 2839–2846, Sep. 2015, doi: 10.1016/j.patcog.2015.03.009.

[56] R. Kohavi, *A Study of Cross-Validation and Bootstrap for Accuracy Estimation and Model Selection*, vol. 14, Mar. 2001. [Online]. Available: https://www.ijcai.org/Proceedings/95-2/Papers/016.pdf

[57] *Data Mining: Practical Machine Learning Tools and Techniques*, Elsevier, Amsterdam, The Netherlands, 2011.

[58] J. R. Quinlan, "Learning decision tree classifiers," *ACM Comput. Surv.*, vol. 28, no. 1, pp. 71–72, Mar. 1996.

[59] L. Breiman, "Random Forests," *Mach. Learn.*, vol. 45, no. 1, pp. 5–32, 2001, doi: 10.1023/a:1010933404324.

[60] W. S. Noble, "What is a support vector machine?" *Nature Biotechnol.*, vol. 24, no. 12, pp. 1565–1567, Dec. 2006, doi: 10.1038/nbt1206-1565.

[61] I. Rish, "An empirical study of the naive Bayes classifier," in *Proc. IJCAI Workshop Empirical Methods Artif. Intell.*, 2001, pp. 1–20.

[62] R. Kohavi and D. Sommerfield, "Feature subset selection using the wrapper method: Overfltting and dynamic search space topology," in *Proc. 1st Int. Conf. Knowl. Discovery Data Mining*, 1995, pp. 192–197.

[63] A. Jovic, K. Brkic, and N. Bogunovic, "A review of feature selection methods with applications," in *Proc. 38th Int. Conv. Inf. Commun. Technol., Electron. Microelectron. (MIPRO)*, May 2015, pp. 1200–1205, doi: 10.1109/MIPRO.2015.7160458.

[64] M. Hossin and M. N. Sulaiman, "A review on evaluation metrics for data classification evaluations," *Int. J. Data Mining Knowl. Manage. Process*, vol. 5, no. 2, pp. 1–11, Mar. 2015, doi: 10.5121/ijdkp.2015.5201.

[65] I. Fatokun et al., "Dual-task gait and white matter hyperintensities in lewy body diseases: An exploratory analysis," *Frontiers Aging Neurosci.*, vol. 15, Apr. 2023, Art. no. 1088050, doi: 10.3389/fnagi.2023.1088050.

[66] J. Michels et al., "Long-term cognitive decline related to the motor phenotype in Parkinson's disease," *J. Parkinson's Disease*, vol. 12, no. 3, pp. 905–916, Apr. 2022, doi: 10.3233/jpd-212787.

[67] J. Perry, J. M. Burnfield, and L. M. Cabico, "Gait analysis: Normal and pathological function," *J. Sports Sci. Med.*, vol. 9, p. 353, Jun. 2010.

[68] H. H. Buddhadev and P. E. Martin, "Effects of age and physical activity status on redistribution of joint work during walking," *Gait Posture*, vol. 50, pp. 131–136, Oct. 2016, doi: 10.1016/j.gaitpost.2016.08.034.

[69] T. Hortobágyi, P. Rider, A. H. Gruber, and P. DeVita, "Age and muscle strength mediate the age-related biomechanical plasticity of gait," *Eur. J. Appl. Physiol.*, vol. 116, no. 4, pp. 805–814, Apr. 2016, doi: 10.1007/s00421-015-3312-8.

[70] D. Kuhman, K. G. Hammond, and C. P. Hurt, "Altered joint kinetic strategies of healthy older adults and individuals with Parkinson's disease to walk at faster speeds," *J. Biomechanics*, vol. 79, pp. 112–118, Oct. 2018, doi: 10.1016/j.jbiomech.2018.07.038.

[71] J. B. Webster and B. J. Darter, "Principles of normal and pathologic gait," in *Atlas of Orthoses and Assistive Devices*. Amsterdam, The Netherlands: Elsevier, 2019, pp. 49–62.

[72] A. Subotic et al., "Gray matter loss relates to dual task gait in lewy body disorders and aging," *J. Neurol.*, vol. 271, no. 2, pp. 962–975, Feb. 2024, doi: 10.1007/s00415-023-12052-y.

Open Access funding provided by 'Università degli Studi di Napoli "Federico II"'
within the CRUI CARE Agreement